A Novel LSTM for Predicting Transmission Line Faults under Ice Disasters

Gengchen Li
School of Electrical Engineering
Northeast Electric Power University
Jilin, China
605544372@qq.com

Tao Jiang
School of Electrical Engineering
Northeast Electric Power University
Jilin, China
t.jiang@aliyun.com

Jindong Cui
School of Economics and Management
Northeast Electric Power University
Jilin, China
jindong1106@sohu.com

Changjiang Wang
School of Electrical Engineering
Northeast Electric Power University
Jilin, China
cjwang17@aliyun.com

***Abstract*—During severe ice disasters, the excessive buildup of ice can cause transmission line failures, greatly undermining the reliability of the power system. This paper investigates the mechanism by which ice disasters affect transmission lines and proposes a prediction method for transmission line fault probability under ice disasters, referred to as MFFA-LSTM. This method plays a key role in addressing the resilience issues of power systems. Through two sets of simulation experiments, it has been verified that the proposed method offers faster computational speed compared to traditional model-driven approaches for calculating line fault rates, while also demonstrating superior prediction accuracy over other LSTM variants.**

Keywords—LSTM, ice disasters, prediction, resilience, transmission system

I. Introduction

The transmission lines play a crucial role in power systems. In recent years, as the global climate continues to deteriorate, extreme ice disasters have become more frequent worldwide, posing severe threats to the stability and reliability of power systems. The occurrence of ice disasters causes significant damage to power systems[1]. In January 2008, southern China was hit by a severe ice disaster, resulting in nearly 129,000 instances of high-voltage line breaks and causing economic losses of 10.45 billion yuan[2,3]. Such incidents illustrate that ice disasters readily result in extensive line failures within power systems, thereby posing a significant threat to their safe and reliable operation. Thus, by predicting the likelihood of transmission line failures caused by ice disasters through the analysis of meteorological data and other pertinent information, it becomes possible to formulate suitable strategies for enhancing resilience. These strategies can help alleviate the effects of ice disasters on the safe and reliable functioning of power systems.

In traditional model-driven approaches, physical equations and models are typically used to describe the behavior of transmission lines under ice and snow conditions. Jones created a model for ice accretion to forecast the buildup of ice on cylindrical structures, which is utilized to evaluate the impact on transmission lines[4]. Brostrom, on the other hand, incorporated variables like wind velocity, precipitation rate, and ice layer thickness to construct a model for analyzing ice disaster impacts[5]. Although these methods perform well in some cases, they often rely on precise physical parameters and assumptions, which are difficult to obtain or contain uncertainties in real-world applications. Moreover, due to the complexity of power systems, traditional model-driven methods struggle to handle large-scale data and complex nonlinear relationships. When extreme weather is about to occur, computational speed becomes a crucial indicator, and traditional model-driven methods often fail to meet these demands. Thus, it is vital to seek a more adaptive predictive method suitable for the real-world conditions of power systems.

With the advancement of artificial intelligence, machine learning algorithms have been applied across various fields to solve practical problems. This paper presents Long Short-Term Memory (LSTM) as a viable solution to address the shortcomings of conventional methods. LSTM, a specific type of Recurrent Neural Network (RNN), has gained popularity in engineering fields because of its effectiveness in capturing long-term dependencies within sequences[6]. Muhammed used three different model architectures—LSTM, CNN-LSTM, and Conv-LSTM—to predict the stability of power system[7]. Heo proposed HT-LSTM, a method that enhances the recognition capability of load types and effectively addresses the issue of low load identification accuracy[8].

Compared with traditional model-driven methods, LSTM demonstrates higher computational speed. However, this method has limitations. The performance of LSTM depends on hyperparameter settings, such as learning rate, batch size, and the number of hidden layer elements. If the hyperparameters are not set properly, the LSTM model may become unstable. Furthermore, although LSTM is designed to alleviate the vanishing gradient problem of traditional RNN, it may still encounter issues in certain special cases, affecting the training effectiveness. Therefore, proper hyperparameter tuning is key to ensuring the performance of LSTM. Optimizing these hyperparameters can enhance the model's accuracy, stability, and efficiency. To tackle this challenge, this paper introduces Male and Female Firefly Algorithm (MFFA) and uses it to optimize the key hyperparameters of LSTM. This leads to the development of the MFFA-LSTM model, which is aimed at predicting the fault probability of transmission lines during ice disasters. First, the characteristics of the traditional Firefly Algorithm (FA) are analyzed, and MFFA is proposed. Then, MFFA is used to optimize the LSTM, creating the MFFA-LSTM model to overcome the shortcomings of traditional models. Finally, the MFFA-LSTM is integrated into the topic studied in this paper. Through two comparative experiments, the accuracy and computational speed of proposed method are verified.

II. A Prediction Model for Transmission Lines Fault Probability

A. Model-driven Transmission Line Fault Probability Model under Ice Disaster

This paper has created a model to evaluate the accumulation of ice thickness on these lines, as well as a fault probability model tailored to transmission lines subjected to icy conditions. Utilizing the spatiotemporal characteristics of such disasters, we created a mathematical framework to

2024 IEEE PES 16th Asia-Pacific Power and Energy Engineering Conference (APPEEC) | 979-8-3503-8612-7/24/$31.00 ©2024 IEEE | DOI: 10.1109/APPEEC61255.2024.10922543

simulate ice disaster scenarios and analyze their impact on transmission systems. This framework also allows us to compute changes in ice thickness along the transmission lines. The model for ice thickness growth is founded on the Jones model[4].

$$D_{\text{ice}}(t)=\frac{1}{\pi\rho_{\text{I}}}\sqrt{\left(\varphi(t)\rho_{\text{W}}\right)^2+(3.6v_wW(t))^2} \quad (1)$$

In (1), $D_{\text{ice}}(t)$ represents the thickness of ice, while $\varphi(t)$ denotes the amount of freezing rain at time t. The symbols ρ_{I} and ρ_{W} indicate the densities of ice and water, respectively, and $W(t)=0.067\cdot\varphi(t)^{0.864}$ signifies the moisture content in the surrounding air.

During icing events on the line, the overall load is influenced by the combined impacts of the vertical ice load L_{I} and the horizontal wind load L_{W}. The vertical load arises from the weight of the ice, whereas the horizontal load is affected by the wind speed in the surrounding area. This relationship is illustrated in Fig. 1.

The ice load $L_{\text{I}}(t)$ is determined by the thickness of ice that has accumulated on the electric cable at a given t.

$$L_{\text{I}}(t)=9.8\times10^{-3}\rho_{\text{I}}\pi\left(d+D_{\text{ice}}(t)\right)D_{\text{ice}}(t) \quad (2)$$

In (2), d signifies the line's diameter.

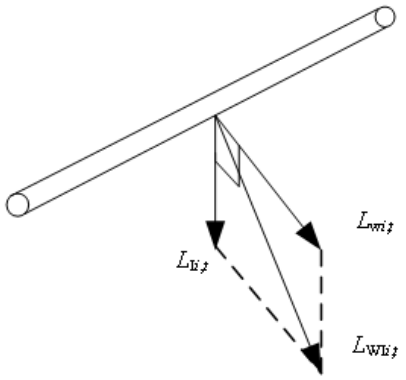

Fig. 1. Illustration of Ice Wind Load on Transmission Lines.

The equation typically used to calculate the wind load is as follows.

$$L_{\text{W}}(t)=CSv_{\text{w}}^2(t)\left(d+2D_{\text{ice}}(t)\right) \quad (3)$$

In (3), C is a constant with a value of $6.964*10^{-3}$; S is the span factor.

$$S=\begin{cases}1-\left(v_{\text{w}}-2.2352\right)\times10^{-3} & v_{\text{w}}>2.2352\text{m/s}\\ 1 & v_{\text{w}}\le2.2352\text{m/s}\end{cases} \quad (4)$$

$v_{\text{w}}(t)$ is the wind speed.

$$v_{\text{w}}(t)=v_{\max}\text{e}^{-\frac{\left(\lambda(t)-\lambda_{\max}\right)^2+\left(\delta(t)-\delta_{\max}\right)^2}{k}}\sin\phi(t) \quad (5)$$

In (5), $v_{\max}$ represents the highest wind speed present in the current environment. $\lambda(t)$ and $\delta(t)$ are the polar radius and polar angle of the transmission line with respect to the center of the ice disaster. $\lambda_{\max}$ and $\delta_{\max}$ are the polar longitude and polar angle of the location with maximum wind speed relative to the center of the ice disaster. ϕ(t) is the angle formed by the line and the direction of the wind, and k is a coefficient.

Thus, the ice wind load per unit length on the transmission line, denoted as ($L_{\text{IW}}(t)$), is given by:

$$L_{\text{IW}}(t)=\sqrt{L_{\text{I}}^2(t)+L_{\text{W}}^2(t)} \quad (6)$$

When constructing a transmission system, it is common to consider the climatic conditions and historical weather data of the region in order to select appropriate design standards for the transmission lines. This ensures that the transmission lines have a certain level of disaster resistance. Based on the design standards, two thresholds for calculating the line failure rate, a_{IW} and b_{IW}, are determined. These thresholds represent the design load capacity and the ultimate load capacity for ice accumulation on the line, respectively. When the line experiences an ice wind load $L_{\text{IW}}(t)<a_{\text{IW}}$, the occurrence of line breakage failures will definitely not happen, meaning the failure rate $P_{\text{f}}(t)=0$. When $a_{\text{IW}}<L_{\text{IW}}(t)<b_{\text{IW}}$, the failure rate for line breakage will increase with the increase in the ice wind load. When $L_{\text{IW}}(t)>b_{\text{IW}}$, the accumulation of ice on the line has exceeded its ultimate load capacity, leading to line breakage failures, meaning $P_{\text{f}}(t)=1$. Thus, based on the ice wind load $L_{\text{IW}}(t)$ that the line is subjected to, as well as the design and ultimate load capacities for ice accumulation, the failure rate $P_{\text{f}}(t)$ for line breakage at time t is determined as follows.

$$P_{\text{f}}(t)=\begin{cases}0 & L_{\text{IW}}(t)\le a_{\text{IW}}\\ e^{\left[\frac{0.6931\left(L_{\text{IW}}(t)-a_{\text{IW}}\right)}{b_{\text{IW}}-a_{\text{IW}}}\right]}-1 & a_{\text{IW}}<L_{\text{IW}}(t)<b_{\text{IW}}\\ 1 & L_{\text{IW}}(t)\ge b_{\text{IW}}\end{cases} \quad (7)$$

The failure rate $P_l(t)$ of a transmission line of length l under ice disaster conditions is as follows.

$$P_l(t)=1-\left(1-P_{\text{f}}(t)\right)^l \quad (8)$$

B. Male and Female Firefly Algorithm(MFFA)

During the analysis of traditional FA performance, it was observed that firefly individuals tend to be attracted to those with better fitness function values, resulting in movement within the solution space. This phenomenon of attraction in optimization algorithms may result in premature convergence, limiting the solution's diversity and effectiveness. In MFFA, the total population size is represented as N, with an equal distribution of male and female fireflies, each accounting for 50% of the total. The male fireflies are denoted as M_i, while the female fireflies are denoted as F_j. Initially, all fireflies are generated randomly to establish the initial population for MFFA, with half assigned as male and the other half as female. Based on this gender classification, the male and female fireflies employ two distinct methods for updating their positions. This gender-based approach is intended to reflect

biological differences, thereby enhancing the efficiency of the algorithm during the search process.

1) Method for updating the location of male fireflies: Considering that male fireflies have a faster movement speed, making it easier for them to find the light of other fireflies located at a distance, a new position update method for male fireflies has been designed based on this characteristic. Since excessive attractiveness may lead to premature convergence, a neighborhood attraction model has been applied to the population of male fireflies. The position update formula has been modified to incorporate a minimum attractiveness parameter, $\beta_{\min}$, which ensures that two male fireflies do not stray too far apart, thereby preventing the attractiveness term from becoming ineffective. Additionally, the disturbance term introduces a scale for the design variables, enhancing the chances that male fireflies will explore further distances. As a result, this approach equips male fireflies with improved global search abilities. Following this analysis, the method for updating the positions of male fireflies is formulated as follows.

$$\begin{aligned} M_j(t+1) &= M_j(t) + \beta_1 * \left(M_i(t) - M_j(t)\right) \\ &+ \alpha_1(t) * h * \left(\varepsilon_j - 0.5\right) \end{aligned} \tag{9}$$

In (9), β_1 represents attractiveness experienced by the male firefly, $\beta_1 \in [\beta_{\min}, \beta_{\max}]$. α_1 represents the step length factor for male fireflies as they move to different positions, h is defined as the length scale, whereas ε_j is a vector within the interval [0,1]. The equations for β_1 and α_1 are as follows.

$$\beta_1 = \beta_{min} + \left(\beta_{max} - \beta_{min}\right) e^{-\gamma r_{ij}^2} \tag{10}$$

$$\alpha_1(t+1) = \alpha_1(t)\, s_1 \tag{11}$$

In (10) and (11), r_{ij} represents the distance separating male firefly i from male firefly j, γ is a coefficient, and the update method for the coordination coefficient s_1 is as follows.

$$s_1 = \frac{1}{2}\left(1 + \frac{t}{iter_{max}}\right) \tag{12}$$

In (12), $iter_{\max}$ is the maximum iteration count of the algorithm.

2) Method for updating the location of female fireflies: From a bionic standpoint, female fireflies exhibit slower movement compared to their male fireflies. Leveraging this characteristic, a novel position update approach for female fireflies has been developed to enhance local search capabilities. Each female firefly is drawn toward the individual, A_{best}, within the population that possesses the highest fitness value. This means that female fireflies are capable of extracting more significant information from superior solutions, thus enhancing their updates in position. Based on this analysis, the method for calculating position updates for female fireflies is outlined as follows.

$$\begin{aligned} F_j(t+1) &= F_j(t) + \beta_2 * \left(F_i(t) - F_j(t)\right) \\ &+ \phi * \left(A_{best}(t) - F_j(t)\right) + \alpha_2(t) * \left(\varepsilon_j - 0.5\right) \end{aligned} \tag{13}$$

β_2 is the attractiveness experienced by the female firefly, α_2 represents the step length factor for female fireflies as they move to different positions, and ϕ is the guiding factor. The updates for β_2, α_2 and ϕ are as follows.

$$\beta_2 = 0.01 + \frac{1}{1 + e^{\left(40\frac{t}{iter_{max}}\right) - 20}} \tag{14}$$

$$\alpha_2(t+1) = \alpha_2(t)\, s_2 \tag{15}$$

$$\phi = \varphi s_2 \tag{16}$$

The calculation equations for s_2 is designed as follows.

$$s_2 = e^{-20\left(\frac{t}{iter_{max}}\right)^{\lambda}} \tag{17}$$

By combining these two position update strategies, a more balanced improvement in both the exploration and exploitation capabilities of the MFFA can be achieved, leading to enhanced overall performance. Once the algorithm has completed its maximum allowable iterations, referred to as $ter_{\max}$, it will present the solution associated with the individual that has achieved the highest fitness value. In other words, this indicates the conclusion of the algorithm, highlighting the best result discovered during the iterations.

C. Fault Probability Prediction Model for Transmission Lines Based on MFFA-LSTM

LSTM, developed by Hochreiter and Schmidhuber in 1997, features a core element known as the cell. This cell includes three key control mechanisms: the Forget Gate, the Input Gate, and the Output Gate. The detailed computational flow is described as follows.

- Input Data.

It takes in the input sequence x_t, the hidden state from the previous time step h_{t-1}, and the cell state C_{t-1}.

- The computation of the Forget Gate.

The Forget Gate is computed using the sigmoid activation function, which helps identify the portions of the cell state that should be removed. This gate is essential for regulating the flow of information within the LSTM cell, as it assesses the significance of the current cell state content that may need to be discarded.

$$f_t = \sigma\left(W_f \cdot \left[h_{t-1}, x_t\right] + b_f\right) \tag{18}$$

- The computation of the Input Gate.

The Input Gate utilizes the sigmoid activation function to decide the new information to be added to the cell state. This gate is crucial for managing the flow of incoming data,

allowing the LSTM cell to retain pertinent information while discarding irrelevant data.

$$i_t = \sigma\left(W_i \cdot \left[h_{t-1}, x_t\right] + b_i\right) \tag{19}$$

$$\tilde{C}_t = tanh\left(W_C \cdot \left[h_{t-1}, x_t\right] + b_C\right) \tag{20}$$

- Update the cell state.

Update the cell state based on the outputs of the Forget Gate and Input Gate.

$$C_t = f_t \cdot C_{t-1} + i_t \cdot \tilde{C}_t \tag{21}$$

- The computation of the Output Gate.

Calculate the Output Gate using the sigmoid activation function to determine the hidden state at the current time step.

$$o_t = \sigma\left(W_o \cdot \left[h_{t-1}, x_t\right] + b_o\right) \tag{22}$$

$$h_t = o_t \cdot tanh\left(C_t\right) \tag{23}$$

- Output the hidden state.

Output the current hidden state h_t as the input for the next iteration.

After modeling MFFA and LSTM, the Mean Squared Error (*MSE*) serves as a fitness function to assess the discrepancy between the predictions made by the model and the actual outcomes. The equation is as follows.

$$MSE = \frac{1}{N}\sum\left(y_k - \hat{y}_k\right)^2 \tag{24}$$

In (24), N refers to the number of samples, y_k stands for the true value of the k-th sample, and $\hat{y}_k$ represents its predicted value.

A smaller value of *MSE* indicates that the model's predictions are closer to the actual results, reflecting better prediction performance.

Due to the high requirements for the settings of certain key hyperparameters in traditional LSTM. Inappropriate configurations of key hyperparameters—such as the learning rate, batch size, and the number of hidden layer units—can lead to poor prediction accuracy and stability in the LSTM model. The learning rate directly affects the model's convergence speed and stability; the batch size influences the model's generalization ability and training efficiency; while the number of hidden layer elements, if set too few or too many, can lead to underfitting or overfitting. These undesirable situations are what we aim to avoid.

Based on this reason, this paper introduces MFFA to effectively search the hyperparameter space and obtain the optimal combination of hyperparameters, thereby proposing the MFFA-LSTM model to improve the model's overall performance. Next, a large number of disaster parameter combinations and their corresponding fault probabilities for transmission lines are used to establish the dataset. The fault rate is calculated using the model-driven approach, and after dividing the dataset into training and testing sets, it is fed into the MFFA-LSTM model for training. Ultimately, the proposed model results in a fault probability prediction model for transmission lines based on MFFA-LSTM model after training. Fig. 2 depicts the scheme of the specific prediction model.

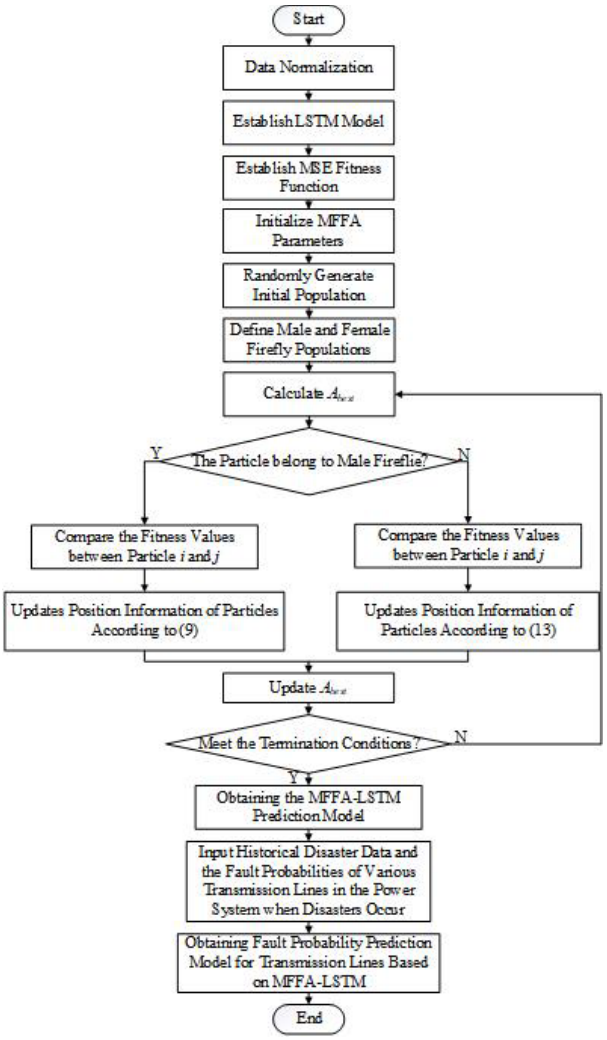

Fig. 2. The Flowchart of MFFA-LSTM.

The operation will cease when the prediction accuracy of the MFFA-BPNN model for estimating transmission line fault probability meets the specified criteria, or when the maximum number of iterations has been achieved. At this point, the final prediction results will be generated and presented.

III. Simulation Experiments and Results Analysis

This study conducts a simulation analysis and validation using the IEEE RTS 79-bus system as a case study, which comprises 24 buses and 38 transmission lines. The dataset used in the simulation experiments is derived from the results obtained using the data-driven model, containing 10000 sets of data. The dataset is meticulously divided into training and testing sets in a 4:1 ratio. This division is used to train MFFA-LSTM model for predicting line fault probabilities. This model is compared with traditional LSTM[6], FA-based LSTM (FA-LSTM)[9], and PSO-based LSTM (PSO-LSTM)[10]. The specific model parameters are set and recorded in Table I.

TABLE I. KEY PARAMETER CONFIGURATION

Algorithm		
PSO	***FA***	***MFFA***
$pop = 80$ $iter_{max} = 1000$ $c_1 = c_2 = 2$ $\omega = 0.9$	$pop = 80$ $iter_{max} = 1000$ $\beta_0 = 1$ $\gamma = 1$	$pop = 80$ $iter_{max} = 1000$ $\gamma = 1$

A. Experimental Results of Prediction Accuracy

This series of simulation experiments employs *MSE* as the metric to assess the prediction accuracy of MFFA-LSTM within the IEEE RTS 79 test system, in comparison with three other models. Table II shows the results.

TABLE II. MSE COMPARISON EXPERIMENTAL RESULTS

Results	Model			
	LSTM	***FA-LSTM***	***PSO-LSTM***	***MFFA-LSTM***
MSE	0.0189	0.0098	0.0103	0.0067

B. Experimental Results of Prediction Efficiency

Simulation experiments were conducted on the testing system using traditional model-driven methods to determine the line failure rate. The prediction time required for the MFFA-LSTM method was compared to verify the speed of this approach. A total of 1000 sets of data from the test set were used for comparison, and the results were averaged.

The computation time for the traditional model-based approach to estimate the electric cable failure rate of the IEEE RTS 79 system during an ice disaster was recorded and averaged. These results were then compared with MFFA-LSTM prediction method, and the findings are presented in Table III.

TABLE III. TIME COMPARISON EXPERIMENTAL RESULTS

Results	Model	
	Traditional model-driven	***MFFA-LSTM***
calculation time	577.61s	0.0883s

The experimental results above indicate that MFFA-LSTM model meets the required prediction accuracy, while the computational efficiency has improved by 99.984% compared to traditional model-driven methods.

IV. CONCLUSION

The repercussions of extreme natural disasters on power systems are critical, as they disrupt the continuity of electricity supply and challenge the resilience of infrastructure, often leading to widespread outages and considerable asset losses. This paper examines the characteristics of traditional FA and formulates a new algorithm called MFFA. This algorithm is used to improve the standard LSTM, resulting in the proposal of the MMFA-LSTM predictive model, which effectively alleviates the issues of low prediction accuracy and poor model stability faced by traditional model. After analyzing the impact of ice disasters, this paper employs the MMFA-LSTM to predict the fault probability of these lines. Finally, through a series of simulations, the predictive performance of four different LSTM models and the efficiency of the proposed method is evaluated by compared to traditional approaches, demonstrating its superiority.

REFERENCES

[1] R. Cloutier, A. Bergeron, and J. Brochu, “On-load network de-icer specification for a large transmission network,” IEEE transactions on power delivery. vol. 22, pp. 1947–1955, June 2007.

[2] W. Zhang, Y. Yu, Z. Su, J. Fan, P. Li, and et al, “Investigation and analysis of icing and snowing disaster happened in Hunan power grid in 2008,” Power System Technology. vol. 32, pp. 1-5, April 2008.

[3] H. Bian, J. Zhang, R. Li, H. Zhao, X. Wang, and Y. Bai, “Risk analysis of tripping accidents of power grid caused by typical natural hazards based on FTA-BN model,” Natural hazards. vol. 106, pp. 1771-1795, April 2021.

[4] K. Jones, “A simple model for freezing rain ice loads,” Atmospheric research. vol. 46, pp. 1-2, April 1998.

[5] E. Brostrom, J. Ahlberg, and L. Soder, “Modelling of ice storms and their impact applied to a part of the Swedish transmission network,” IEEE Lausanne Power Tech. pp. 1593-1598, July 2007.

[6] J. Schmidhuber, and S. Hochreiter, “Long short-term memory,” Neural Comput. vol. 9, pp. 1735-1780, November 1997.

[7] A. Muhammed, Y. Isbeih, M. El Moursi, and K. Al Hosani, “Deep learning-based models for predicting poorly damped low-frequency modes of oscillations,” IEEE Transactions on Power Systems. vol. 39, pp. 3257-3270, May 2024.

[8] T. Le, S. Heo, and H. Kim, “Toward load identification based on the Hilbert transform and sequence to sequence long short-term memory,” IEEE Transactions on Smart Grid. vol. 12, pp. 3252-3264, July 2021.

[9] Y. Cong, X. Zhao, K. Tang, G. Wang, Y. Hu, and et al, “FA-LSTM: A novel toxic gas concentration prediction model in pollutant environment,” IEEE Access. vol. 10, pp. 1591-1602, January 2022.

[10] X. Ren, S. Liu, X. Yu, and X. Dong, “A method for state-of-charge estimation of lithium-ion batteries based on PSO-LSTM,” Energy. vol. 234, pp. 121236, November 2021.